

Attic Ventilation Model

T.W. Forest, P.Eng.
Member ASHRAE

I.S. Walker

ABSTRACT

An attic ventilation model has been developed based on equating the mass flow rate of air into and out of an enclosed attic space. Attic airflows are driven by a combination of temperature- (stack effect) and wind-induced pressure differences. Inputs to the model are the leakage characteristics of the attic, attic and ambient temperatures, wind speed, and wind direction. Predicted ventilation rates are compared with measured data from two separate attics that have been monitored over the past two years. One attic had no intentional openings and correspondingly low ventilation rates, while the second attic had soffit and roof vents and high ventilation rates. The model predictions showed reasonably good agreement with the measured data, particularly the dependence of ventilation rate on wind speed and wind direction.

INTRODUCTION

The attics of most residential houses are enclosed spaces that are generally well insulated from the interior conditioned portion of the house. With the high levels of ceiling insulation that are now quite common, the attic space is subjected to extreme cold during winter and heat during summer. In addition to the large temperature swings that can occur in an attic, any moisture that enters, either by exfiltration of humid indoor air into the attic or by external rain or snow infiltration, can accumulate and cause problems, such as structural deterioration of wood trusses and roof sheathing and growth of microorganisms. Building codes have recognized these potential problems and require some means of providing ventilation of attics with outdoor air. The standard code specification is a total attic vent area equal to 1/300th of the attic floor area. Several questions arise from this code requirement: (1) How much ventilation is provided by these vent openings? (2) Do certain vent configurations provide more ventilation than others? (3) Is there an optimum level of ventilation to control temperature and moisture in attics? The code provides no answers to these questions.

One avenue of approach has been the development of mathematical models to simulate the thermal and moisture dynamics in attics. Examples of models for simulating the thermal performance of attics are those developed by Wilkes (1989, 1991), which include a ventilation model; Abrantes (1985); and Peavy (1979). Simulations of attic moisture performance have been developed by Gorman (1987), Ford (1982), and Burch and Luna (1980); the

moisture models, of necessity, incorporated thermal models of the attic since the mass transfer processes associated with moisture flows are dependent on the thermal balance within the attic. In most of these models, the attic ventilation rate is either specified as a user input or as empirical data. Since the thermal and moisture models are dependent on ventilation rates, these models by themselves are somewhat limited when used to simulate the seasonal performance of an attic. Generally, the variation of ventilation rate with wind speed and wind direction for a particular attic is not available, and only rough estimates of ventilation rates have been used.

The current study was undertaken to develop an attic ventilation model and to verify the model with sufficient field data on well-characterized attics. The ventilation model is based on balancing the mass flow of air (induced by stack and wind pressures) into and out of an attic. The model is capable of incorporating intentional openings in the attic, such as roof and soffit vents, as well as unintentional leakage, such as small cracks and holes associated with attic construction. Model predictions were compared with ventilation rates that were measured in two separate attics—one with no intentional vent openings and the other with soffits and two flush-mounted roof vents. Given the scatter in the measured data, the predicted ventilation rates showed reasonably good agreement with measured data. The model was able to predict the measured dependence of ventilation rates on wind speed and wind direction. The ultimate objective of this work will be to integrate this ventilation model with the available attic thermal and moisture models.

ATTIC VENTILATION MODEL

Prediction of attic ventilation rates is based on an airflow mass balance of the enclosed attic volume. The key assumptions of the model are that the attic air is well mixed (implying no significant temperature gradients in the air), the background leakage (excluding site-specific vent openings) can be uniformly distributed over a surface, and the airflow through the attic is quasi-steady. Since the ventilation rate predictions are to be compared with hourly averaged measurements, the last assumption is justified.

Consider a leakage site located on the outer envelope of an enclosed attic space, as shown in Figure 1. The pressure difference across this leakage site is a combination of the stack- and wind-induced pressure differences and can be expressed as

Tom Forest is a professor and Iain Walker is a Ph.D. candidate in the Department of Mechanical Engineering, University of Alberta, Edmonton, Alberta, Canada.

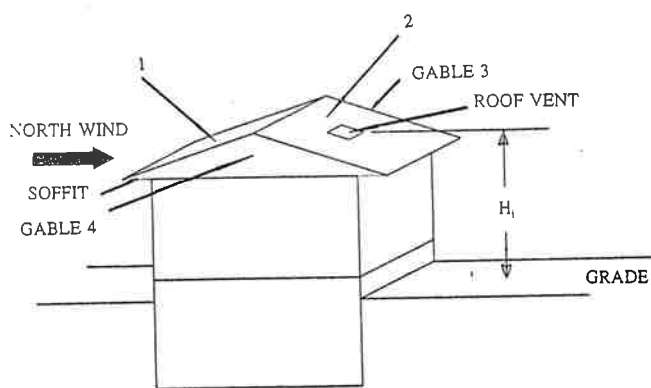


Figure 1 Schematic of gable-end attic showing numbered sequence for attic surfaces.

$$\Delta P_i = \Delta P_{ref} - \Delta T_p H_i + \Delta P_w C_{pi} S_{wi}^2 \quad (1)$$

where

- ΔP_i = outdoor-attic pressure difference (defined as positive when outdoor pressure is greater than attic pressure),
 H_i = height of leakage site above grade,
 C_{pi} = exterior wind pressure coefficient for leakage site (referenced to the wind speed at the eave height), and
 S_{wi} = shelter factor for leakage site.

The shelter factor is a dimensionless ratio that multiplies the wind speed at the height of the eaves to account for shelter due to neighboring obstacles; the magnitude of S_{wi} is between 0 and 1, with 0 referring to complete shelter (i.e., no wind pressures on the attic) and 1 referring to no shelter. The two factors ΔT_p and ΔP_w are defined as

$$\Delta T_p \equiv \rho_\infty g \frac{T_A - T_\infty}{T_A}$$

$$\Delta P_w \equiv \rho_\infty \frac{U^2}{2}$$

where

- ρ_∞ = ambient air density,
 g = gravitational constant,
 U = wind speed at the eave height,
 T_A = attic air temperature, and
 T_∞ = ambient air temperature.

The term ΔP_{ref} in Equation 1 is the unknown reference outdoor-attic pressure difference at zero height (at grade level) that must be calculated from the mass flow rate balance. It should be noted that the stack- and wind-induced pressures are *not* additive but interact through this unknown reference pressure difference.

Wind Pressure Coefficients

Since the principal driving force for attic ventilation is wind-induced pressure on the attic, it is important that the wind pressure coefficients, C_p , be determined as accurately as possible. For the gable-end attic tested (shown in Figure 1), pressure coefficients on the two sloped sections of the roof, gable ends, and soffits were determined from the measurements made by Wiren (1984) and those reported by Liddament (1986). For wind directions normal to the roof ridge, the pressure coefficients on the upwind and downwind sloped roof sections, $C_p(1)$ and $C_p(2)$ (labeled as surfaces 1 and 2, respectively, in Figure 1), are given in Table 1. For low sloped roofs, the pressure coefficients have negative values, which implies that the entire roof surface is within a separated flow region. For higher sloped roofs, airflow is attached to the upwind section, giving positive pressure coefficients while flow separation occurs at the roof ridge. When the wind direction changes by 90° so that flow is parallel to the roof ridge, the pressure coefficients on the sloped sections depend on whether the house is isolated or is part of a row of houses. In this attic model, it is assumed that for wind directions parallel to the roof ridge, the sloped roof pressure coefficients behave in the same way as the vertical walls of the house. For the two vertical sections of a house parallel to the flow (labeled as surfaces 3 and 4 in Figure 1), Akins et al. (1979) measured a pressure coefficient of -0.65 for an isolated house; for row houses, -0.2 is used, as these surfaces are in the wake of upstream houses (Wiren 1984). From these limiting values for C_p , a harmonic trigonometric interpolation function was developed to obtain C_p values for varying wind directions:

$$C_p(\theta) = \frac{1}{2} [(C_p(1) + C_p(2)) \cos^2 \theta + (C_p(1) - C_p(2)) F + (C_p(3) + C_p(4)) \sin^2 \theta + (C_p(3) - C_p(4)) \sin \theta] \quad (2)$$

where

- θ = the angle between the roof section line and a line normal to the wind direction measured in a clockwise direction.

The effect of roof pitch, α , is contained in the factor, F , and is defined as

$$F = \frac{1 - |(\cos \theta)^5|}{2} \left[\left| \frac{28^\circ - \alpha}{28^\circ} \right|^{0.01} + \frac{1 + |(\cos \theta)^5|}{2} \right]$$

The factor, F , is close to 1 for a roof pitch between 0 and 28° ; at a larger roof pitch, F behaves approximately as $\cos \theta$. Figure 2 shows the trigonometric interpolation function when the roof pitch is in the range of 10° to 30° ; the measured ventilation rates, reported in the following section, were taken in attics with a roof pitch of 18.4° . It should be emphasized that these data are for the sloped roof sections of the attic envelope. The pressure coefficients on the gable ends were assumed to be the same as the pressure

TABLE 1
Wind Pressure Coefficients on the Upwind
and Downwind Sections of Sloped Roofs

Roof Pitch α	Pressure Coefficients	
	Upwind, $C_p(1)$	Downwind, $C_p(2)$
< 10°	-0.8	-0.4
10° to 30°	-0.4	-0.4
> 30°	0.3	-0.5

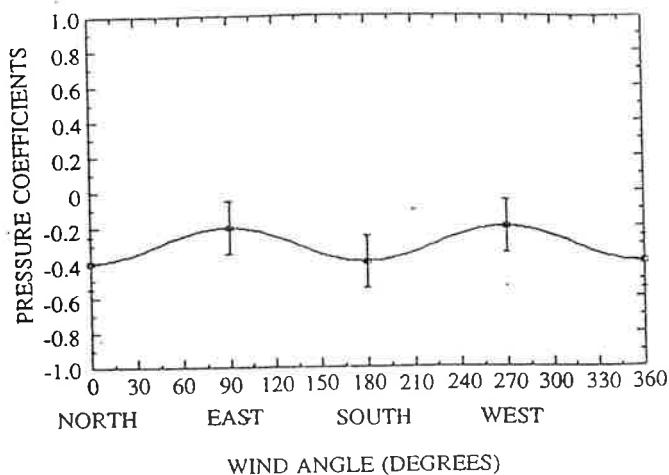


Figure 2 Variation of pressure coefficients on low-sloped roofs of houses in a row vs. wind angle. Data for pitch angles between 10° and 30°. — trigonometric interpolation function.

coefficients on the vertical walls of the house since the gables are simply an extension of the walls. A similar trigonometric interpolation approach was used to fit the pressure coefficient data of Akins et al. (1979) for vertical walls of houses. Finally, the pressure coefficients on the eaves (where soffit vents can be located) were assumed to be the same as those on the vertical wall beneath the eaves. In the absence of any detailed measurements of these pressure coefficients, this was the most reasonable assumption. In applying these pressure coefficients in the ventilation model, it was assumed that the pressure coefficient on each section of the attic envelope was a constant over that entire section. Again, lack of detailed information on pressure coefficient distributions on a particular section precludes incorporation of this effect in the model. Also, such detail would make the ventilation model more complex than it needs to be at this time.

Wind Shelter

Obstacles surrounding the attic produce a reduction in wind speed at the building due to the obstacle's wake. This effect can be expressed as a wind reduction factor or shelter factor, S_w , which varies between 0 (complete shelter) and 1 (unsheltered). The method used to generate the shelter factors is based on a new wind-shadow technique and will only be briefly outlined in this section. The theory and complete development of this technique will be the subject of a forthcoming publication by Wilson and Walker. In this model, upwind obstacles create a wake of mean velocity defect. The shelter factor is obtained by projecting the wind "shadow" of an upwind obstruction on a particular surface of a building and calculating the wind reduction at that surface. The model also takes into account the effect of fluctuating wind directions due to turbulence by assuming a Gaussian distribution for wind direction. An example of the wind shelter function is shown in Figure 3 for the north wall of one of the test houses used in the field study. The attic ventilation model assumes that the shelter factor for the sloped roof sections is the same as for the wall section beneath it. In each of the figures, the shelter factors decrease significantly for wind directions where the neighboring houses in the east-west row provide shelter.

Calculation of Ventilation Flow Rates

Attic ventilation rates are calculated by balancing the mass flow rate of air into and out of the attic. The output of this calculation is the unknown value of ΔP_{rep} which balances the inflows and outflows. The mass flow rate of air through leakage site i , \dot{m}_i , is expressed as

$$\dot{m}_i = \rho_i C_i \Delta P_i^{n_i} \quad (3)$$

where

ρ_i = density of ambient air— ρ_∞ for inflow or ρ_A for outflow,

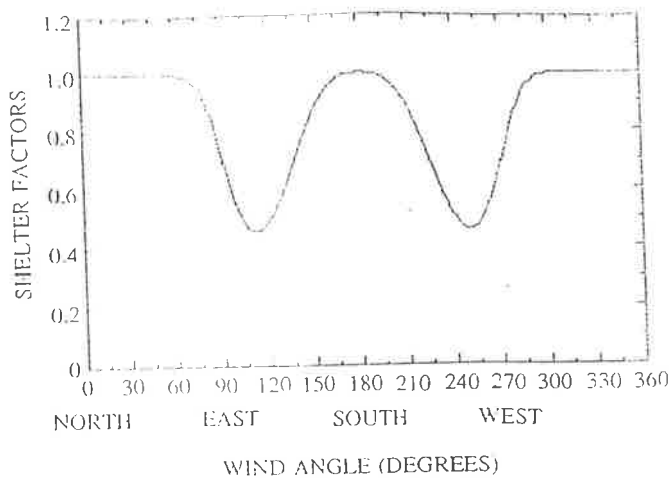


Figure 3 Shelter factor for the north face of houses in a row vs. wind angle.

C_i = flow coefficient of each leak, and
 n_i = flow exponent of each leak.

The leakage sites on the attic envelope can be separated into unintentional openings, such as tiny cracks and holes, and intentional openings, such as roof vents, soffits, etc. Note that a positive mass flow rate is defined as flow into the attic when $\Delta P_i > 0$ and vice versa when $\Delta P_i < 0$.

The unintentional leakage is assumed to be distributed uniformly over the roof surfaces, and the flow through each surface is found by integrating the pressure difference over the height of that surface. Since different densities are applied to inflows and outflows, these must be calculated separately. The boundary between inflows and outflows is the height at which the attic pressure and outdoor pressure are equal. The height of this boundary above grade is the neutral height, H_{NL} , which can be expressed as

$$H_{NL} = \frac{(\Delta P_{ref} + \Delta P_w C_p S_w^2)}{\Delta T_p} \quad (4)$$

Note that the pressure coefficient and shelter factor are constant over the entire surface under consideration, and the neutral height must be calculated separately for each surface of the attic envelope. Several cases exist, depending on the attic-outdoor temperature difference and the neutral height.

Attic-Outdoor Temperature Difference Zero In the limit when there is no attic-outdoor temperature difference, ΔT_p is zero and the neutral height is undefined. In this case, there is no variation in pressure with height and the flow on the particular roof surface will be in or out, depending on the wind pressures. For a given pressure difference, ΔP , given by Equation 1, the mass flow rates are

$$\begin{aligned} \dot{m}_{out} &= \rho_A C_{roof} \Delta P^n & \Delta P < 0 \\ \dot{m}_{in} &= \rho_\infty C_{roof} \Delta P^n & \Delta P > 0 \end{aligned}$$

where C_{roof} refers to the flow coefficient of the particular surface of the roof being considered.

Attic-Outdoor Temperature Difference Not Zero In this case, the pressure varies with height, h (measured relative to grade), which implies that the airflow varies over the surface of interest. The incremental mass flow rate, $d\dot{m}$, over height, dh , of the surface is

$$d\dot{m}(h) = \rho \Delta P^n(h) dC_{roof} \quad (5)$$

where ΔP is calculated using Equation 1 with H_i set equal to h . The incremental flow coefficient of the roof surface, dC_{roof} , can be expressed as

$$dC_{roof} = \frac{C_{roof}}{H_p - H_e} dh \quad (6)$$

where

H_p = height of the roof peak above grade,
 H_e = height of eaves above grade.

The expression for dC_{roof} follows from the assumption of uniform distribution of leakage area over the roof surface. The mass flow rate for a particular roof surface is found by integrating Equation 5. However, the limits of integration depend on the neutral height. The first case is when the attic temperature is greater than the outdoor temperature. If the neutral height lies between H_p and H_e , the mass flows in and out are

$$\dot{m}_{in} = \frac{\rho_\infty C_{roof} \Delta P_2^{n+1}}{(H_p - H_e) \Delta T_p^{n+1}} \quad (7a)$$

and

$$\dot{m}_{out} = \frac{\rho_A C_{roof} \Delta P_1^{n+1}}{(H_p - H_e) \Delta T_p^{n+1}} \quad (7b)$$

where ΔP_1 and ΔP_2 are calculated using Equation 1 with H_i set equal to H_p and H_e , respectively; if the entire roof surface is above the neutral height, then mass flow out across the surface is

$$\dot{m}_{out} = \frac{\rho_A C_{roof} (\Delta P_1^{n+1} - \Delta P_2^{n+1})}{(H_p - H_e) \Delta T_p^{n+1}}; \quad (8)$$

if the entire roof surface is below the neutral height, the mass flow in across the surface is

$$\dot{m}_{in} = \frac{\rho_\infty C_{roof} (\Delta P_1^{n+1} - \Delta P_2^{n+1})}{(H_p - H_e) \Delta T_p^{n+1}} \quad (9)$$

The second case is when the attic temperature is less than the outdoor temperature. If the neutral height lies between H_p and H_e , then ΔP_2 is replaced by $-\Delta P_1$ in Equation 7a and ΔP_1 is replaced by $-\Delta P_2$ in Equation 7b; if the entire surface is above the neutral level, the mass

flow of air into the attic is given by Equation 9, with the pressure difference term $\Delta P_1^{n+1} - \Delta P_2^{n+1}$ multiplied by -1 ; if the entire roof surface is below the neutral level, the mass flow of air out of the attic is given by Equation 8, with the same pressure difference term multiplied by -1 .

For intentional openings whose height above grade, H_i , is known, the pressure difference is given by Equation 1. The mass flow of air through these leakage sites is then

$$\dot{m}_i = \rho C_i \left(\frac{T_{ref}}{T} \right)^{3n_i - 2} \Delta P_i^{n_i} \quad (10)$$

where

$$T_{ref} = 527.67 \text{ if } T \text{ is degrees Rankine,}$$

$$T_{ref} = 293.15 \text{ if } T \text{ is degrees Kelvin.}$$

The air density and temperature are evaluated at the ambient or attic conditions, depending on whether the flow is into or out of the attic. The C_i and n_i are the leakage characteristics of the vent at 68°F (20°C), and the temperature ratio term in Equation 10 is a correction factor to account for the variation of air density and viscosity with temperature.

Model Calculation Procedure

For given ambient temperature, wind speed, and direction, the mass flow rates through each surface of the attic envelope are formulated according to the procedures set out in the previous section. The only unknown in these equations is ΔP_{ref} . An iterative procedure is used to solve for this pressure difference by initially assigning a value of zero. Mass flow rates for all surfaces of the attic envelope are calculated; if the sum of the inflows does not equal the sum of the outflows, then a new value is selected using a binary search method where the change in ΔP_{ref} is halved at each iteration. This procedure is repeated until the change in ΔP_{ref} is less than 4×10^{-7} in. w.c. (0.0001 Pa). Once the solution has converged, the attic ventilation rate is the final sum of the inflows (which is equal to the sum of outflows).

COMPARISON OF MEASURED AND PREDICTED ATTIC VENTILATION RATES

The ventilation rates in two separately configured attics are currently being measured over a two-year span that started in December 1990. Measurements were performed in two unoccupied houses at a research facility located near Edmonton, Alberta, Canada; details of the test facility are described by Gilpin et al. (1980). The houses selected are two of six identical houses arranged in an east-west row; each house is a single-story construction with full basement and has plan measurements of 22 ft by 24 ft (6.7 m by 7.3 m). The roof design has gable ends with a full-length ridge oriented along the east-west direction. The roof pitch is 3 to 1 (with $\alpha = 18.4^\circ$), and the heels of the roof trusses are

raised 2.5 ft (0.67 m) to allow for added ceiling insulation. The total enclosed attic volume is estimated to be 2,154 ft³ (61 m³). The two houses selected (houses 5 and 6) are the last two houses on the east end of the row, and the leakage distribution in each attic was configured differently. The two leakage configurations tested were a "tight" construction with no vent openings and a "loose" construction with soffits and roof vents. Attic 5 was selected as the tight attic with no intentional vents; the only leakage area was the background leakage of the roof sheathing and gable ends. Attic 6 was fitted with soffit vents along the north and south eaves and two flush-mounted attic vents, one on the south-sloped roof section and one on the north section. A photograph of houses 5 and 6 is shown in Figure 4. For attic 6, the soffits were mounted on "false" eaves that were aligned with the floor of the attic; this was done to have the soffit leakage area in a location that was representative of conventional residential construction. The leakage characteristics of each attic were measured by a two-zone blower test. The interior of the attic was depressurized, while the pressure difference between the house and attic was maintained at zero by a second blower connecting the interior with the outdoors. Thus, the measured leakage area represents the total attic envelope leakage area excluding the ceiling. The results of these leakage tests are given in Table 2. Leakage tests on attic 6 were carried out with the two roof vents closed but soffits left open. For the ventilation model, these measured leakage characteristics were taken to be that corresponding to the background leakage of each attic. For attic 6, each roof vent had a gross area of 55.8 in.² (0.036 m²) and was located 14.8 ft (4.5 m) above grade. Attic ventilation rates were measured using a constant-concentration tracer gas technique. Details of the measurement system and data analysis will not be discussed here but are given in a report by Forest et al. (1991).

Attic Ventilation Rates

The measured ventilation rates in attics 5 and 6 are shown in Figures 5a and 5b, respectively, as a function of



Figure 4 Photograph of houses 5 (on right) and 6 (on left) at AHHRF. Note the false eaves just above the center window of house 6.

TABLE 2
Attic Leakage Characteristics
of Attics 5 and 6 from Depressurization Tests
 $Q = C(\Delta P)^n$

Attic	Flow coefficient, C		Flow Exponent, n	Leakage Area, A _L , at 0.016 "WC (4 Pa)	
	ft ³ /min/"WC ⁿ	m ³ /s(Pa) ⁿ		in. ²	m ²
5	4.638x10 ³	4.416x10 ⁻²	0.707	70.6	4.557x10 ⁻²
6 ¹	9.955x10 ³	1.740x10 ⁻¹	0.597	239.1	1.542x10 ⁻¹

¹ Measured with attic roof vents closed but soffits left open.

Note: "WC = inches of water column.

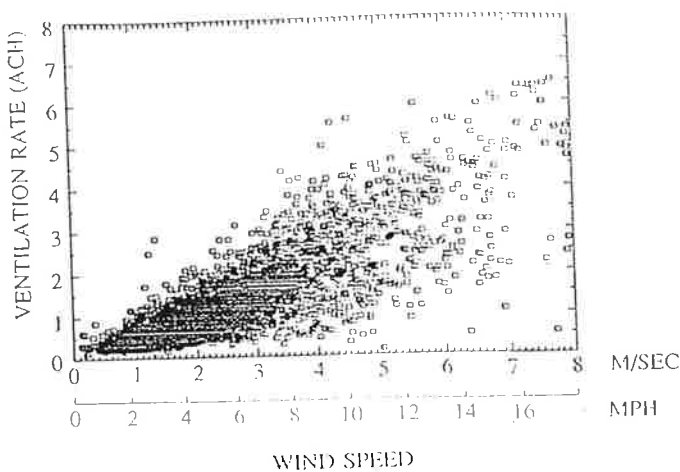


Figure 5a Measured hourly averaged ventilation rate (ach) vs. wind speed for attic 5. Data set contains 3,758 data points.

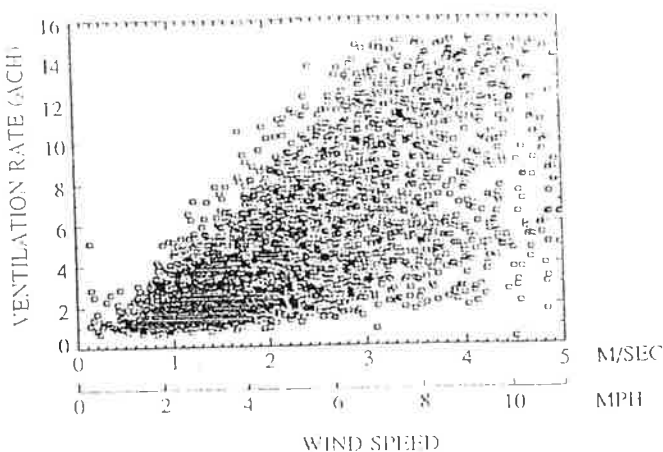


Figure 5b Measured hourly averaged ventilation rates (ach) vs. wind speed for attic 6. Data set contains 3,522 data points.

wind speed. These data were selected from the time period between March 1 and October 31, 1991, and encompass all wind directions; totals of 3,758 and 3,522 hourly averaged data points are included in Figures 5a and 5b, respectively. Note that ventilation rates in attic 5 are much less than in attic 6 and reflect the difference in leakage areas of the two attics, attic 5 having approximately one-third the leakage area of attic 6. The data set for attic 6 (Figure 5b) extends up to a maximum average wind speed of approximately 11 mph (5 m/s) as compared to 18 mph (8 m/s) for attic 5. At these high wind speeds, the ventilation rate in attic 6 approaches 20 (ach), which has been determined to be the upper limit of the tracer gas system used in this study.

Both sets of data show a general increase in ventilation rate with wind speed, although there is considerable scatter in these data. A large part of this scatter is due to changing wind direction, which alters both the shelter and pressure coefficients of the attics. Both attics are essentially unsheltered for winds from the north or south and would therefore have large ventilation rates, while strong shelter occurs for east and west winds, thus producing lower ventilation rates. An example of this is shown in Figures 6a and 6b, where attic 5 ventilation rates are shown as a function of wind speed for north and west winds. Each data set only includes wind directions $\pm 22.5^\circ$ about the nominal direction. For west winds, the ventilation rates are noticeably less than for north winds. The ventilation measurements also showed that attic ventilation rates are not dependent on attic-outdoor temperature differences unless the wind speed is very low; thus, the model predictions, discussed below, are only compared to measured data in terms of wind speed and direction.

Model predictions were made for ventilation rates in both attics. In order to make these predictions, certain assumptions were made regarding leakage distribution over the attic envelope. In most house construction, there will be certain areas where the unintentional leakage area is concentrated. Such areas are the eaves where the sloped

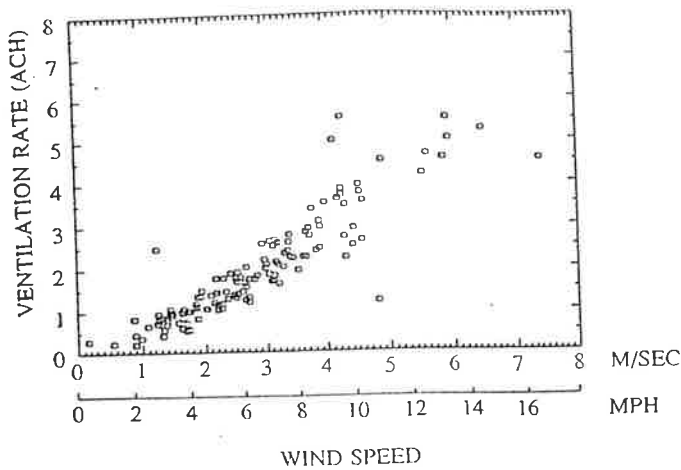


Figure 6a Measured ventilation rates in attic 5 vs. wind speed for wind directions $\pm 22.5^\circ$ about due north.

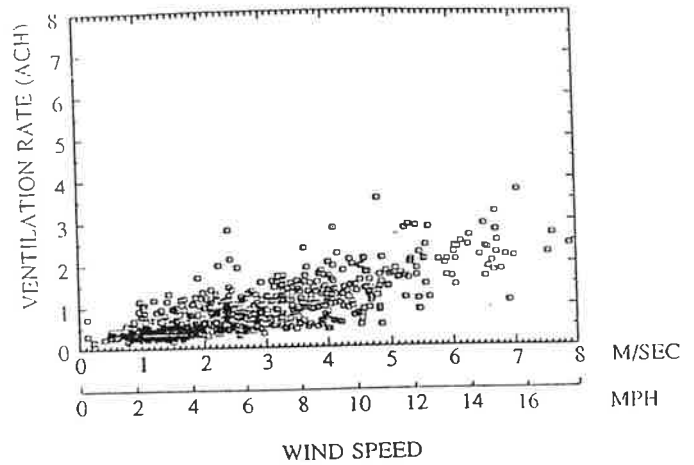


Figure 6b Measured ventilation rates in attic 5 vs. wind speed for wind directions $\pm 22.5^\circ$ about due west.

TABLE 3
Assumed Distribution of Background Leakage Area
and Pertinent Dimensions of Attics 5 and 6

Surface or Point on Attic Envelope ¹	Attic 5		Attic 6	
	%	height above grade, ft (m)	% (or area in bold)	height above grade, ft (m)
Eaves on roof surface 1	25	9.8 (3)	45	9.8 (3)
Eaves on roof surface 2	25	9.8 (3)	45	9.8 (3)
Gable - surface 3	5	13.1 (4)	0	-
Gable - surface 4	5	13.1 (4)	0	-
Roof surface 1	20	distributed	5	distributed
Roof surface 2	20	distributed	5	distributed
Roof peak	-	16.4 (5)	-	16.4 (5)
Vents on roof surface 1	none	-	55.8 in.² (0.036 m²)	14.8 (4.5)
Vents on roof surface 2	none	-	55.8 in.² (0.036 m²)	14.8 (4.5)

¹ Refer to Figure 1 . roof surface reference numbers.

roof sections attach to the vertical walls; another is the joint between the gable walls and the sloped roof sections. Since the blower tests only gave the total leakage area, a reasonable distribution for these unintentional leaks was assumed, and a summary of the leakage distribution and pertinent dimensions of each attic is presented in Table 3. The C and n values for each attic were taken from Table 2. For attic

6, the two roof vents were treated separately as a leakage site with $C = (\text{discharge coefficient} = 0.6) \times (\text{gross vent area})$ and $n = 0.5$; the vents are assumed to behave like orifices with turbulent flow through them. The predicted and measured ventilation rates are shown in Figures 7a and 7b versus wind speed for all wind directions for attics 5 and 6, respectively. The measured data, shown in Figures 5a

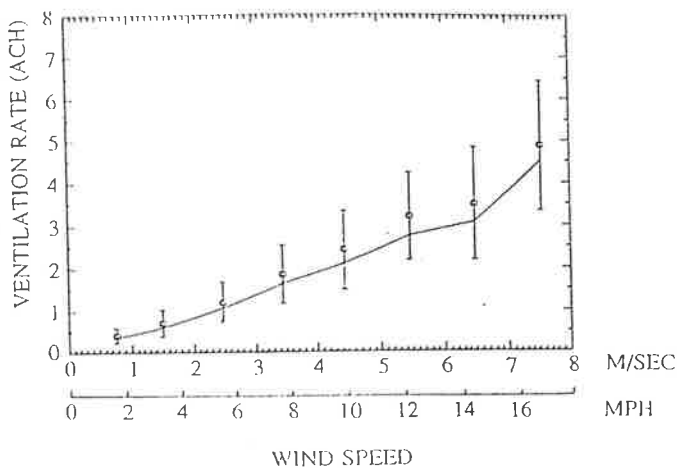


Figure 7a Comparison of predicted and measured ventilation rates in attic 5 vs. wind speed. $\bar{\phi}$ average and one standard deviation in each 2.25-mph (1-m/s) increment of wind speed. — model predictions.

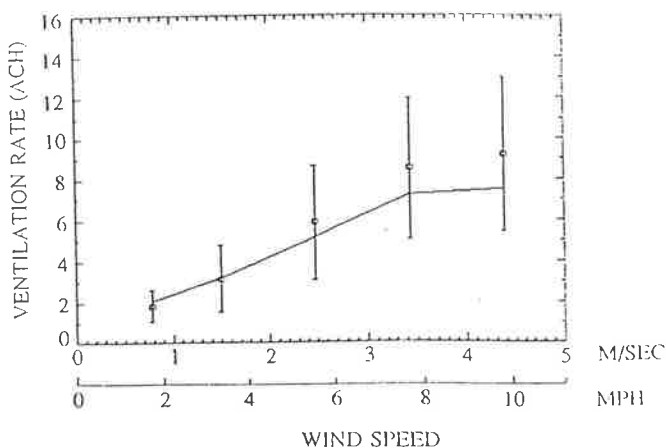


Figure 7b Comparison of predicted and measured ventilation rates in attic 6 vs. wind speed. $\bar{\phi}$ average and one standard deviation in each 2.25-mph (1-m/s) increment of wind speed. — model predictions.

and 5b, have been averaged over each 2.25 mph (1 m/s) increment in wind speed; this average and error bars corresponding to one standard deviation are shown by the square symbols, while the predicted rates are shown by the solid line. Model predictions were made using the measured wind speed, wind direction, and ambient air temperature for each hour. The other input was the attic air temperature, which, of course, depends on the attic ventilation rate. For this portion of the study, the measured attic air temperature was used as input to the ventilation model. Future work will combine the ventilation model with a thermal model of the attic to predict both attic temperature and ventilation rate. The hour-by-hour predictions of ventilation rate resulted in a scattered data set, and these data were averaged to obtain the predicted average value. For both attics 5 and 6, the

model predictions are in reasonable agreement with measured values, although there seems to be some tendency for the model to underpredict the data. This could be due to the pressure coefficients that were used as input. Undoubtedly, the model could be run with the pressure coefficients adjusted slightly to better fit the data; however, this was not done. Model refinement can only occur when more detailed measurements of roof pressure coefficients become available in the literature.

A more stringent test of the model is a comparison between the predicted and measured dependence of ventilation rates on wind direction. This comparison is shown in Figures 8a and 8b for attics 5 and 6, respectively. The

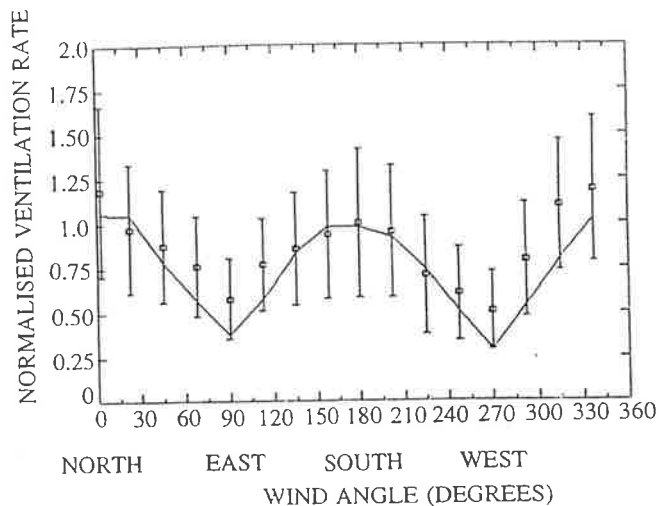


Figure 8a Normalized ventilation rates in attic 5 vs. wind direction. For each wind direction, measured ventilation rates have been divided by U^{2n} . $\bar{\phi}$ average and one standard deviation for measured data. — model predictions.

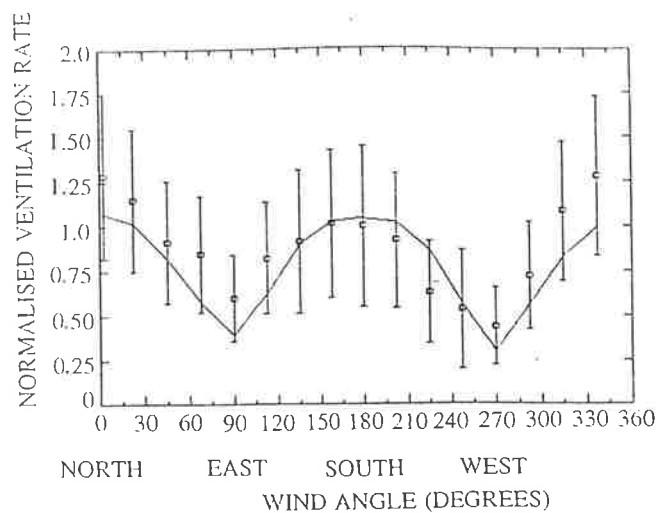


Figure 8b Normalized ventilation rates in attic 6 vs. wind direction. For each wind direction, measured ventilation rates have been divided by U^{2n} . $\bar{\phi}$ average and one standard deviation for measured data. — model predictions.

measured data have been averaged for each 22.5° increment in wind angle. In order to highlight the effect of wind direction on ventilation rates, the data have been normalized by the average ventilation rate for south winds ($\theta = 180^\circ$). In addition, to remove some of the scatter in this data set, each data point was divided by the reference (eave height) wind speed raised to the power $2n$, where n is the flow exponent of the attic; this has the effect of removing the dependence of ventilation rates on wind speed (shown in Figures 7a and 7b). First, the measured data clearly show the variation of ventilation rates with wind direction, particularly when moving from the unsheltered directions, north (0°) and south (180°), to the sheltered directions, east (90°) and west (270°). In attic 5, there is almost a 40% decrease in the average ventilation rate from the unsheltered to the sheltered directions; furthermore, this decrease is approximately the same for both the east and west directions since attic 5 is sheltered from east and west winds by identical houses on either side. In attic 6, the decrease in ventilation rate for west winds is approximately 55% from the unsheltered directions, while the decrease is approximately 40% for east winds. Unlike attic 5, attic 6 is sheltered from west winds by an identical house (house 5), but for east winds, the only shelter is a rectangular vertical wall that is 12.1 ft (3.7 m) high, the same width as the houses, and located 8.5 ft (2.6 m) away from the end of the house. This structure does not provide the same type of shelter as does a neighboring house. The predicted ventilation rates are shown by the solid lines in Figures 8a and 8b and show reasonable agreement with the measured data. In particular, the model is able to predict with reasonable accuracy the variation of ventilation rate with wind angle, although the magnitude of the decrease for the sheltered directions is somewhat larger than the measured data. Again, this may reflect the values of pressure coefficients and/or leakage distribution that are used, and slight variations in these values may improve the predictions.

A detailed analysis of the percent difference between the predicted and measured ventilation rates was carried out for all wind directions together and for each of the principal wind directions separately. The results of this analysis are presented in Table 4. These results clearly show that the model underpredicts the ventilation rates for east-west winds where the attics are sheltered and tends to overpredict (except for north winds on attic 6) for north-south winds where the attics are unsheltered. As mentioned previously, the poorer predictions for sheltered directions may be due to a combination of the values of pressure coefficients used and calculation of the shelter factors using the wind-shadow technique. If all wind directions are used to calculate the overall percent error, the results show smaller errors of -9.3% for attic 5 and +4.3% for attic 6. It should be noted that these results are somewhat dependent on the assumed attic leakage distribution.

SUMMARY AND CONCLUSIONS

A new attic ventilation model has been developed based

on balancing the mass flow rate of air into the attic with mass flow leaving the attic. The mass flow rates of air through distributed leakage on the attic envelope and through intentional vent openings are expressed in terms of the stack- and wind-induced pressure differences; wind shelter has been incorporated using a simple wind-shadow technique. The unknown reference pressure difference, ΔP_{ref} , is calculated iteratively from a mass balance on the attic envelope.

Field measurements of ventilation rates in two separate attics have been taken since December 1990. The attics were identical in construction, except that one had no soffits or attic vents, while the other had soffit vents and two flush-mounted roof vents. A comparison of the measured and predicted attic ventilation rates showed that the model was able to predict all of the important trends observed in the data. Ventilation rates increased with wind speed and the strong dependence of ventilation rate on wind direction; there was a clear decrease in measured and predicted ventilation rates for wind directions in which the attics were strongly sheltered by neighboring houses. Based on the comparison of predicted and measured ventilation rates, it is concluded that the present attic model is able to accurately predict ventilation rates and will be very useful for assessing the effectiveness of various attic ventilation strategies. Future work will be aimed at coupling the ventilation model with a thermal and moisture model of the attic space. This will allow the thermal and moisture performance of an attic to be modeled over a winter heating season.

ACKNOWLEDGMENTS

Support for the field measurements of attic ventilation rates was provided initially through the Alberta/Canada Energy Resource Research Fund (Province of Alberta) and later by Canada Mortgage and Housing Corporation (CMHC), Ottawa, Ontario, Canada. Support for I.S. Walker was provided by R.M. Hardy Engineering Enrichment Fund (University of Alberta); CMHC; Energy, Mines, and Resources (EMR—Government of Canada); and the Natural Sciences and Engineering Research Council (NSERC—Government of Canada).

REFERENCES

- Abrantes, V. 1985. Thermal exchanges through ventilated attics. *Proceedings of the ASHRAE/DOE/BTECC Thermal Performance of the Exterior Envelopes of Buildings III*, Clearwater Beach, pp. 296-308.
- Akins, R.E., J.A. Peterka, and J.E. Cermack. 1979. Averaged pressure coefficients for rectangular buildings. *Wind Engineering—Proceedings of the Fifth International Conference*, vol. 1. Fort Collins, CO.
- Burch, D.M., and D.E. Luna. 1980. A mathematical model for predicting attic ventilation rates required for preventing condensation on roof sheathing. *ASHRAE Transactions* 86(1): 201-212.

TABLE 4
Percent Difference Between the Predicted
and Measured Ventilation Rates for Attics 5 and 6

Wind Direction ¹	Attic 5 %	Attic 6 %
North	+2.2	-14.1
South	+14.2	+18.9
East	-25.8	-27.1
West	-28.8	-17.1
All directions	-9.3	+4.3

1. Includes wind directions $\pm 22.5^\circ$ about the nominal direction

Ford, J.K. 1982. Heat flow and moisture dynamics in a residential attic. Center for Energy and Environmental Studies and PU/CEES Report #148. Princeton, NJ: Princeton University.

Forest, T.W., I.S. Walker, and K. Checkwitsch. 1991. Moisture accumulation in a building envelope—Final report of AHHRF 1989-90 heating season. Report #80. Edmonton: Department of Mechanical Engineering, University of Alberta.

Gilpin, R.R., J.D. Dale, T.W. Forest, and M.Y. Ackerman. 1980. Construction of the Alberta home heating research facility and results for the 1979-1980 heating season. Report #23. Edmonton: Department of Mechanical Engineering, University of Alberta.

Gorman, T.M. 1987. Modeling attic humidity as a function of weather, building construction, and ventilation rates. Ph.D. dissertation, College of Environmental Science and Forestry, State University of New York, Syracuse.

Liddament, M.W. 1986. *Air infiltration calculation techniques—An applications guide*. Berkshire, UK: Air Infiltration and Ventilation Centre.

Peavy, B.A. 1979. A model for predicting the thermal performance of ventilated attics. *Summer Attic and Whole-House Ventilation*, pp. 119-145. NBS Special Publication 548. Gaithersburg, MD: National Institute for Standards and Technology.

Wilkes, K.E. 1989. Thermal modeling of residential attics with radiant barriers: Comparison with laboratory and field data. *Proceedings of the ASHRAE/DOE/BTECC/CIBSE Conference on the Thermal Performance of the Exterior Envelopes of Buildings IV*, pp. 294-311.

Wilkes, K.E. 1991. Thermal model of attic systems with radiant barriers. ORNL/CON-262. Oak Ridge, TN: Oak Ridge National Laboratory.

Wiren, B.G. 1984. Wind pressure distributions and ventilation losses for a single-family house as influenced by surrounding buildings—A wind tunnel study. *Proceedings of the Air Infiltration Centre Wind Pressure Workshop*, Brussels. Berkshire, UK: Air Infiltration and Ventilation Centre.